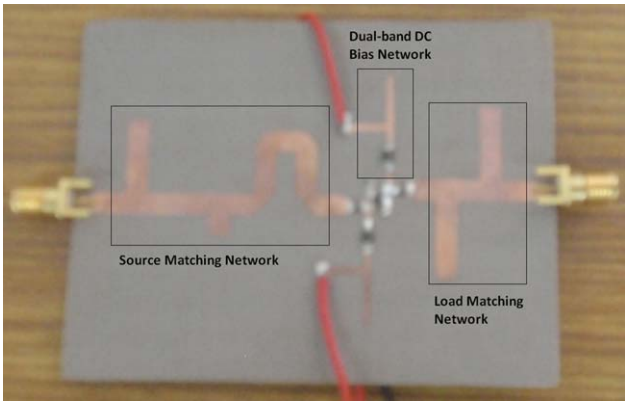

Figure 6 Fabricated concurrent dual-band LNA. [Color figure can be viewed in the online issue, which is available at wileyonlinelibrary.com]

figure is measured with help of Agilent noise figure meter setup. Figure 5 shows simulated and measured noise figure performance. Table 5 summarizes the simulated and measured noise figure performance.

The measurement analysis shows that the proposed concurrent dual-band LNA has fair gain ($S21$) and reasonable NF at both bands. Hence, it can be used as a subsystem for a concurrent dual-band RF system for noninvasive vital sign detection system, as proposed in [4]. Figure 6 shows the fabricated LNA.

4. CONCLUSION

In this article, the concept of a concurrent dual-band LNA with the intention of use as the essential part of a concurrent dual-band RF system for vital sign detection is introduced. The article depicts concurrent dual-band impedance matching characteristics of conventional double open-circuited shunt-stubs structure. A novel methodology is also provided for dual-band concurrent DC bias network. The effectiveness of the proposed methodology is demonstrated through measurement results. Measured performance of the fabricated LNA exhibits the required dual-band response with a wideband rejection in between the two operating frequencies of 2.44 GHz and 5.25 GHz.

REFERENCES

1. C. Li and J. Lin, Random body movement cancellation in Doppler radar vital sign detection, IEEE Trans Microwave Theory Tech 56 (2008), 3143–3152.
2. K.M. Chen, Y. Huang, J. Zhang, and A. Norman, Microwave life-detection systems for searching human subjects under earthquake rubble and behind barrier, IEEE Trans Biomed Eng 47 (2000), 105–114.
3. B. Iyer, M. Garg, N.P. Pathak, and D. Ghosh, Concurrent dual-band RF system for human respiration rate and heartbeat detection, In: Proceedings of ICT-2013, Kanyakumari, Tamil Nadu, India, 2013, pp. 749–753.
4. B. Iyer, M. Garg, N.P. Pathak, and D. Ghosh, Non-invasive detection and analysis of human vital signs using concurrent dual-band RF system, In: IConDM 2013, IIITDM Chennai, India, July 2013.
5. H. Hashemi and A. Hajimiri, Concurrent multiband low-noise amplifiers—theory, design, and applications, IEEE Trans Microwave Theory Tech 50 (2002), 288–301.
6. C. Garg, V. Sharma, and N.P. Pathak, Double shunt stub impedance matching network based concurrent dual-WLAN-band amplifier, In: Proceedings of National Conference on Recent Trends on Microwaves Techniques and Applications, Jodhpur, India, July 31, 2011.

DESIGN OF COMPACT BROADBAND PHASE SHIFTER WITH CONSTANT LOSS VARIATION

Han Lim Lee,[1] Seong-Mo Moon,[2] Moon-Que Lee,[3] and Jong-Won Yu[1]
[1] School of Electrical Engineering and Computer Science, KAIST, 291 Daehak-ro, Yuseong-Gu, Daejeon, South Korea
[2] RF and Satellite Payload Research Team, ETRI, 138 Gajeong-ro, Yuseong-Gu, Daejeon, South Korea
[3] School of Electrical Engineering and Computer Science, UOS, 13 Siripdae-gil, Dongdaemun-Gu, Seoul, South Korea; Corresponding author: mqlee@uos.ac.kr

Received 7 June 2013

ABSTRACT: *Two types of compact broadband phase shifter MMICs (monolithic microwave integrated circuits) with constant insertion loss variations are presented. Both phase shifters are reflection-type phase shifters using a Lange coupler as a 3-dB coupler and LC resonance terminations. The first type phase shifter uses a single diode with reverse biasing as a varactor and adopts a miniaturized Lange coupler to maximize compactness and to minimize parasitic loss. The second type adopts back-to-back connected diodes with reverse biasing as a varactor for wider tunable phase range and parallel resistors for constant insertion loss variation. For both types, MMIC's are fabricated in GaAs 0.15-μm low noise pHEMT (p-high electron mobility transition) process and required indcutances are implemented by microstrip lines. The implemented MMIC phase shifter of the first type shows the measured relative phase shift range of 80° and measured insertion loss of 2.1 ± 0.2 dB at 20 GHz. The measured relative phase shift range of 72 ± 9° and the measured insertion loss variation of ±0.2 dB are obtained from 15 to 25 GHz. Similarly, the second type phase shifter shows the measured relative phase shift range of 104° and measured insertion loss of 2.4 ± 0.1 dB at 21 GHz. Also, the broadband characteristic of the second type is verified by the measured relative phase shift range of 96 ± 8° with the constant insertion loss variation of ±0.2 dB from 17 to 25 GHz.* © 2014 Wiley Periodicals, Inc. Microwave Opt Technol Lett 56:394–400, 2014; View this article online at wileyonlinelibrary.com. DOI 10.1002/mop.28097

Key words: *phase shifter; MMIC; constant loss variation*

1. INTRODUCTION

Phase shifters are one of the most widely used components and take important roles in microwave systems such as phased-array systems, radar systems, and communication systems. Although there have been many researches for enhancement in phase shift range, small insertion loss variation, and device miniaturization by adopting lumped elements coupler [1], slow-wave microstrip lines [2], two quarter-wave transmission lines [3], or series and parallel LC circuits [4], some researches with well-established numerical analysis were conducted only in hybrid form at limited operation frequency band [5, 6]. In these previous works, a 3-dB impedance transforming branch line coupler is combined with LC resonance terminations and parallel resistors for wide phase shift range and constant insertion loss. However, adopting 3-dB impedance transforming branch line coupler restricts the phase shifter's operation band very narrow and consequently the constant insertion loss characteristic by the parallel resistor has not been observed over enough frequency ranges. Also, the independency of insertion loss on reactance variation at high frequencies, where parasitic effects are significant, has not been

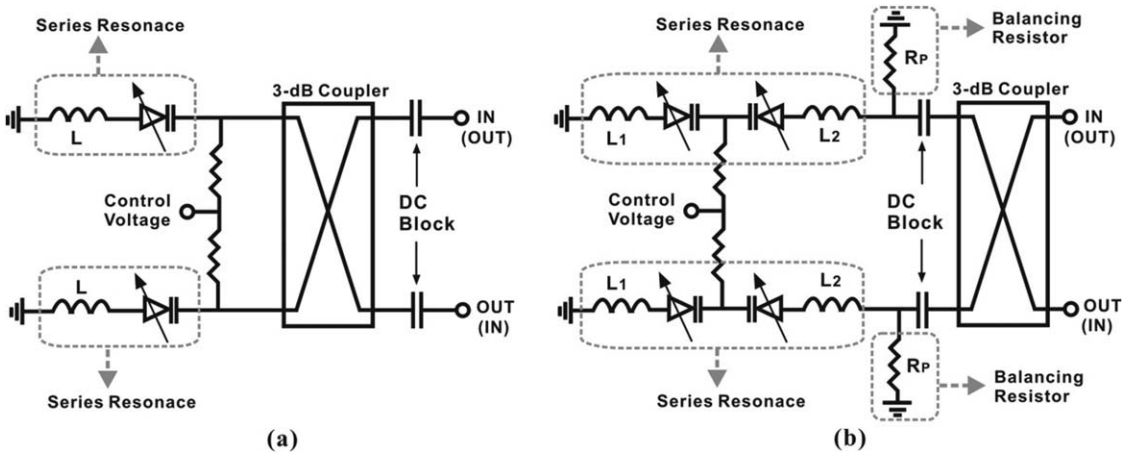

Figure 1 Schematic of the broadband phase shifter with constant loss variation. (a) Type 1. (b) Type 2

examined due to the measurement at relatively low frequencies. Moreover, as the branch-line coupler is not preferable in IC design due to its relatively large size, the use of branch-line coupler might not be practical.

In order to examine the constant loss variation performance by adopting parallel resistors over broadband and high frequency ranges and compare with the performance of the miniaturized phase shifter without parallel resistors, two types of MMIC phase shifters are designed and analyzed in this article. Both types are configured with LC resonance reflective circuits and Lange couplers instead of branch line couplers. The first type uses a miniaturized Lange coupler to maximize the compactness while to minimize the parasitic loss caused by long microstrip lines and large areas. Similarly, the second type uses a Lange coupler but adopts a parallel resistor in resonance circuit to balance the insertion loss variations. For the first and second types, varactors are implemented by a single reverse-biased diode and a back-to-back connected reverse-biased diode, respectively. By adopting a back-to-back diode, wider frequency tuning range can be achieved, but larger circuit size and more parasitic loss are expected comparing to the structure with a single diode as a varactor. By designing these two types of phase shifters, the broadband performance of the phase shifter using constant loss variation techniques, miniaturization, and balancing resistor, can be observed and compared with other reflection type phase shifter IC's implemented in GaAs process with different techniques such as lumped-element coupler [1], branch-line coupler with planar varactor diode [7], optimized reflective circuitry [8], and two resonated loads in parallel [9].

2. BROADBAND PHASE SHIFTER WITH CONSTANT LOSS VARIATION DESIGN

The simplified schematics of the first and second type phase shifters are shown in Figures 1(a) and 1(b), respectively. The 3-dB couplers for both types are Lange couplers but Type 1 uses a miniaturized Lange coupler, whereas Type 2 uses a regular Lange coupler. As shown in Figure 1(a), broadband phase shifter Type 1 adopts a single diode as a varactor without any parallel component added. If the sum of parasitic resistances by varactor and inductor is denoted as R_S and the capacitance by the varactor is indicated as C_V, the reflection coefficient and relative phase for Type 1 can be expressed as follows,

$$\Gamma_L = \frac{(R_S - Z_O) + j(\omega L - 1/\omega C_V)}{(R_S + Z_O) + j(\omega L - 1/\omega C_V)}, \tag{1}$$

$$\phi = \frac{\pi}{2} + \tan^{-1}\left(\frac{\omega L - 1/\omega C_V}{R_S - Z_O}\right) - \tan^{-1}\left(\frac{\omega L - 1/\omega C_V}{R_S + Z_O}\right). \tag{2}$$

As the insertion loss for Type 1 phase shifter is $|\Gamma_L|^2$, the constant insertion loss regardless of the changes in varactor capacitances can be achieved by satisfying Eq. (3),

$$\left|\frac{R_S - Z_O}{R_S + Z_O}\right|^2 = 1. \tag{3}$$

Because $R_S - Z_O$ can never be exactly the same as $R_S + Z_O$, the insertion loss can only be approximated as constant by the assumption of $Z_O \gg R_S$. For $Z_O = 50\ \Omega$, the condition for constant loss variation of Type 1 is optimized by applying the single diode as a varactor and miniaturizing the circuit size to minimize R_S.

For Type 2 phase shifter as shown in Figure 1(b), a back-to-back connected diode as a varactor and a parallel resistor to balance the insertion loss variation are used. As similar as Type 1 phase shifter, if the sum of parasitic resistances by varactor and inductor is denoted as R_S and the capacitance by the varactor is indicated as C_V, the reflection coefficient and relative phase for Type 2 can be expressed as follows,

$$\Gamma_L = \frac{(R_S R_P - R_S Z_O - R_P Z_O) + j\{\omega(L_1 + L_2) - 1/\omega C_V\}(R_P - Z_O)}{(R_S R_P + R_S Z_O + R_P Z_O) + j\{\omega(L_1 + L_2) - 1/\omega C_V\}(R_P + Z_O)}, \tag{4}$$

$$\phi = \frac{\pi}{2} + \tan^{-1}\frac{\{\omega(L_1 + L_2) - 1/\omega C_V\}(R_P - Z_O)}{(R_S R_P - R_S Z_O - R_P Z_O)} - \tan^{-1}\frac{\{\omega(L_1 + L_2) - 1/\omega C_V\}(R_P + Z_O)}{(R_S R_P + R_S Z_O + R_P Z_O)} \tag{5}$$

As the insertion loss for Type 2 phase shifter is $|\Gamma_L|^2$, the constant insertion loss regardless of the changes in varactor capacitances can be achieved by satisfying Eq. (6),

$$\left|\frac{R_S R_P - R_S Z_O - R_P Z_O}{R_S R_P + R_S Z_O + R_P Z_O}\right|^2 = \left|\frac{R_P - Z_O}{R_P + Z_O}\right|^2. \tag{6}$$

Then, the optimum value of R_P can be determined by solving Eq. (6) and given as follows,

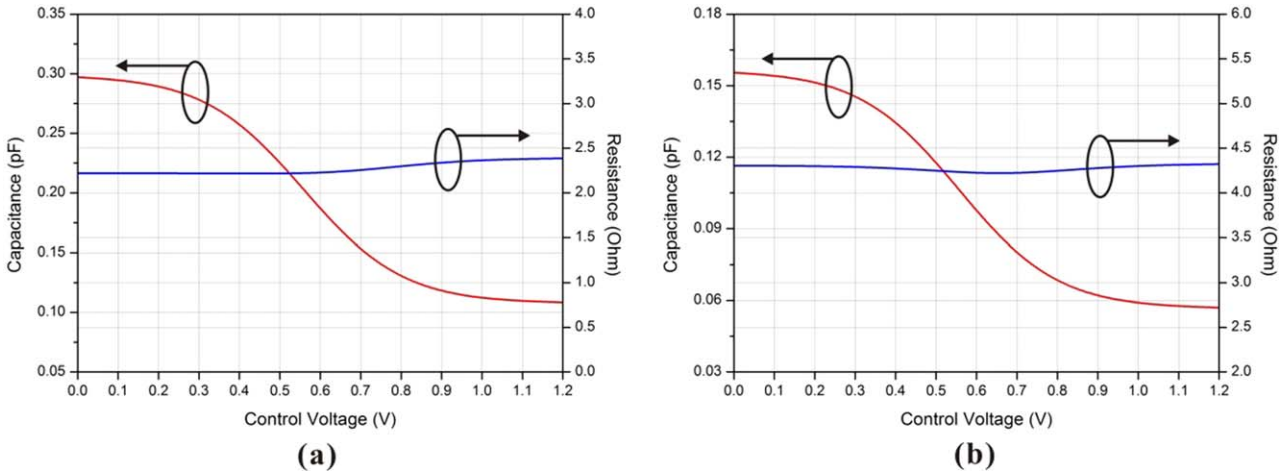

Figure 2 Capacitance and series resistance of varactors for (a) Type 1 and (b) Type 2. [Color figure can be viewed in the online issue, which is available at wileyonlinelibrary.com]

$$R_P = \frac{Z_O^2}{2R_S} \cdot \left\{ 1 + \sqrt{1 + \left(\frac{2R_S}{Z_O} \right)^2} \right\}. \tag{7}$$

Having the optimal R_P, the insertion loss can be theoretically constant as follows,

$$\text{I.L}_{\cdot \text{with } R_P} = \left| \frac{Z_O + \sqrt{Z_O^2 + 4R_S^2} - 2R_S}{Z_O + \sqrt{Z_O^2 + 4R_S^2} + 2R_S} \right|^2. \tag{8}$$

As seen from Eq. (8), the insertion loss is independent of varactor reactance variation which determines the relative phase tuning range of the phase shifter. For Type 1 and Type 2 phase shifters, the relative phase shift ranges can be determined by Eqs. (2) and (5), respectively, with the maximum and minimum varactor capacitances as follows,

$$\Delta\phi = |\phi(C_{V,\max}) - \phi(C_{V,\min})|. \tag{9}$$

Although the resonance by inductance and capacitance by varactor can further increase the phase shift range, the variation ability of varactor capacitance determines the maximum phase shift range for phase shifters as in Eq. (9) as the more resonance used for the increase in phase range, the more insertion loss by the increased resonance the reflection type phase shifter have. Moreover, as the available varactor diode characteristics differ from process to process, the characteristics of varactor diode in given process should be investigated. Figure 2 shows the capacitance variations as well as the series resistances according to control voltages for the varactors adopted by Type 1 and 2 in GaAs 0.15-μm pHEMT process.

The varactor for Type 1 is a reverse-biased single diode with a series resistance of about 2.5 Ω and its capacitance varies from 0.1 to 0.3 pF approximately with respect to the control

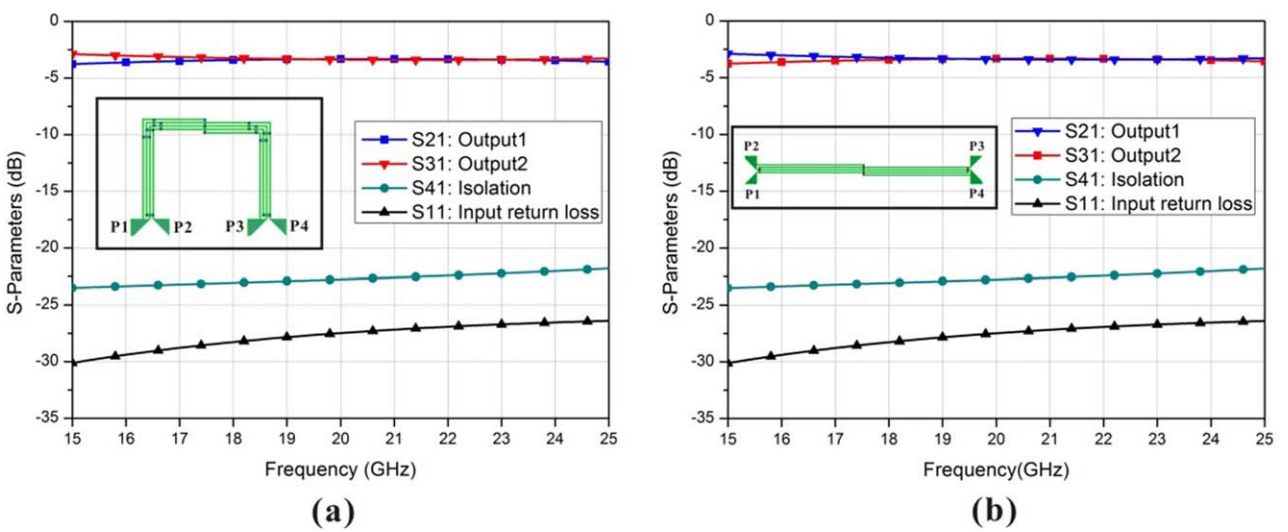

Figure 3 Simulated results for (a) miniaturized Lange coupler and (b) regular Lange coupler from 15 to 25 GHz. [Color figure can be viewed in the online issue, which is available at wileyonlinelibrary.com]

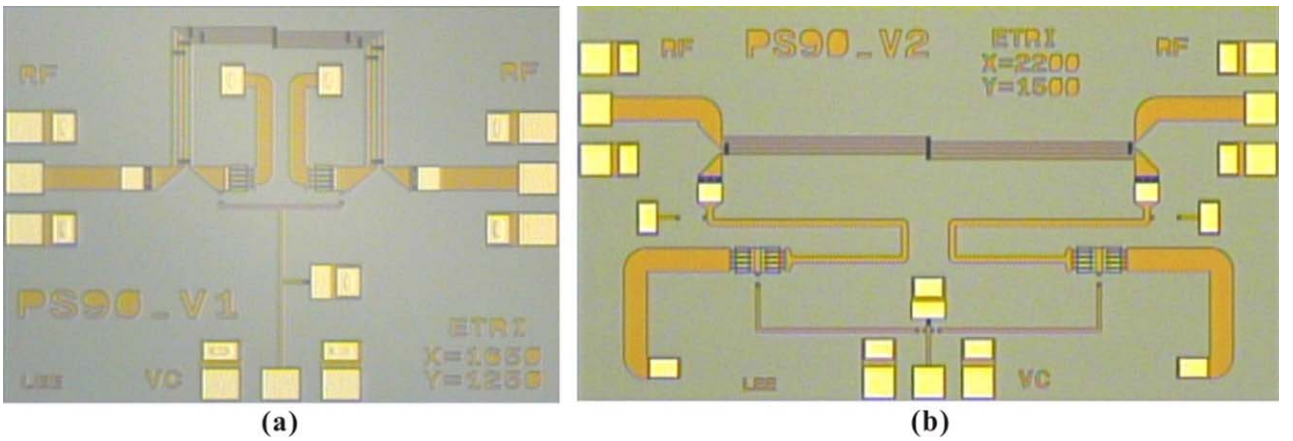

Figure 4 Implemented broadband phase shifter with constant insertion loss variation MMIC for (a) Type 1 and (b) Type 2. [Color figure can be viewed in the online issue, which is available at wileyonlinelibrary.com]

voltages from 0 to 1.2 V. The varactor for Type 2 is a reverse-biased back-to-back connected diode with a series resistance of about 4.5 Ω and its capacitance varies from 0.05 to 0.16 pF approximately with respect to the control voltages from 0 to 1.2 V. As seen from Figure 2, the varactor diodes provide linear variations in capacitances between 0.3 and 0.9 V, but the control voltages outside this range provides very slow changes in capacitances which can be the source of nonlinear phase variation when phase shifters are implemented. Based on the values found from varactor diodes, the required inductances for Type 1 and 2, and a parallel resistor for Type 2 can be approximately determined for initial design.

3. SIMULATION AND MEASUREMENT

For reflection type phase shifters, the performance of 3-dB coupler should first be validated as the input and output return losses of phase shifters are determined by the couplers. Figure 3 shows the simulated results for the miniaturized Lange coupler

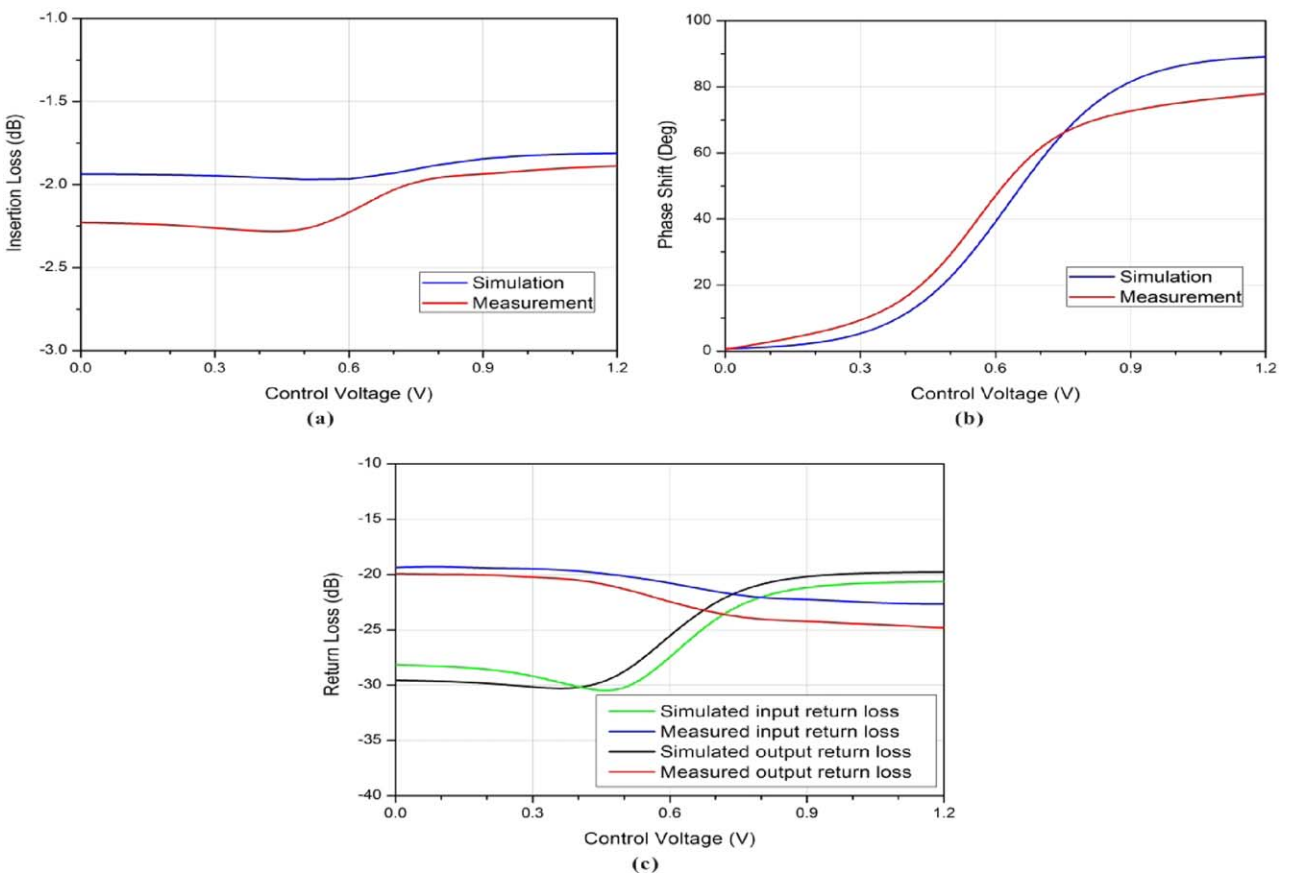

Figure 5 Simulated and measured (a) insertion loss, (b) relative phase shift range, and (c) input and output return losses for MMIC Type 1 at 20 GHz with control voltages from 0 to 1.2 V. [Color figure can be viewed in the online issue, which is available at wileyonlinelibrary.com]

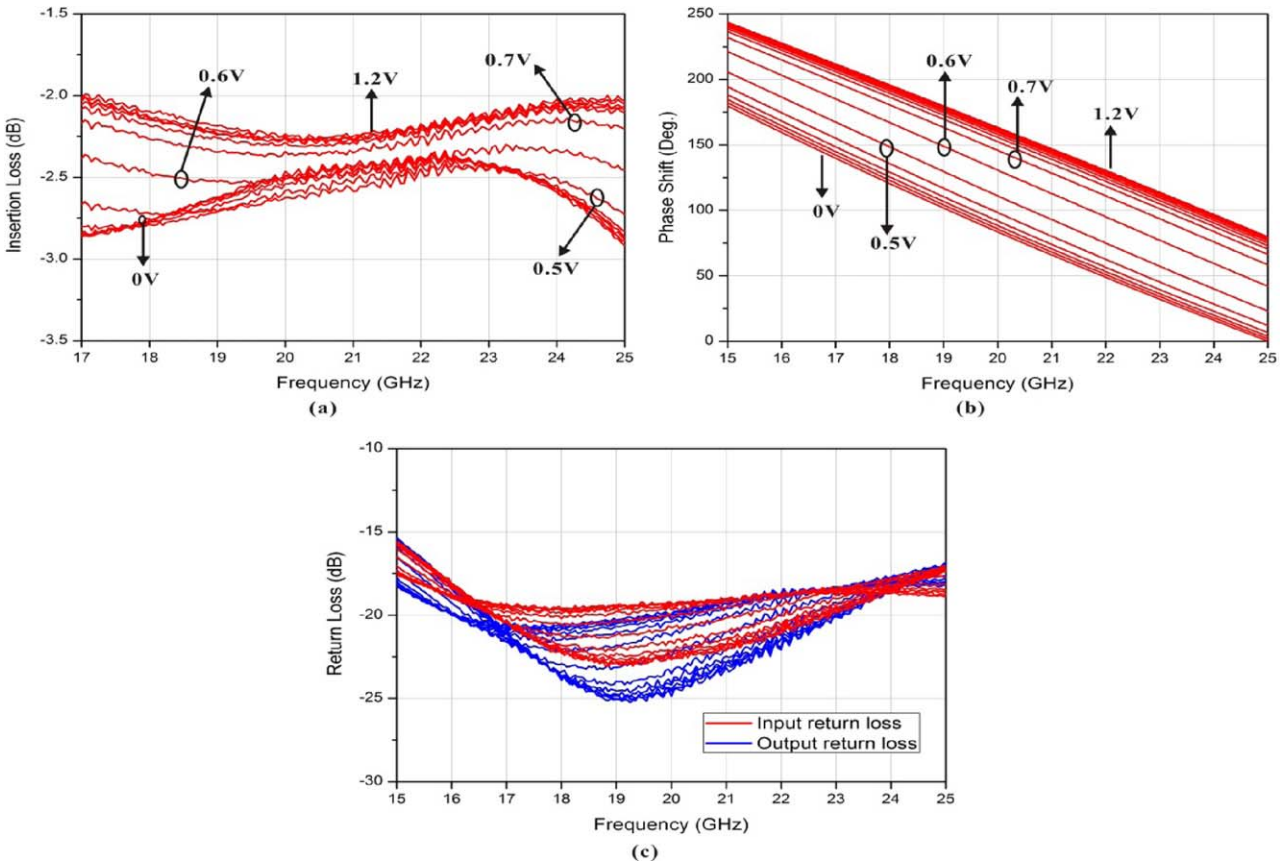

Figure 6 Measured (a) insertion loss, (b) relative phase shift range, and (c) input and output return losses for MMIC Type 1 from 15 to 25 GHz with control voltages from 0 to 1.2 V. [Color figure can be viewed in the online issue, which is available at wileyonlinelibrary.com]

for Type 1 and the regular Lange coupler for Type 2 at high frequencies. The miniaturized Lange coupler has more air-bridge connections among microstrip lines to compensate the imbalance in coupling due to the bending of microstrip lines comparing to the regular Lange coupler. It is noted that the performance of the miniaturized Lange coupler is almost identical to the regular Lange coupler.

For both phase shifters, GaAs 0.15-μm low noise pHEMT process is used for fabrication. Figures 4(a) and 4(b) show the implemented broadband phase shifter MMIC Type 1 and Type 2, respectively. The size of the fabricated phase shifter Type 1 and Type 2 excluding test pads are 820 $\times$ 640 μm^2 and 1900 $\times$ 900 μm^2, respectively. Figure 5 shows the simulated and measured result for Type 1 MMIC according to control voltages. The measured relative phase shift range of 80°, insertion loss of 2.1 ± 0.2 dB, and return losses better than 20 dB were obtained at 20 GHz for control voltage variation from 0 to 1.2 V. For the broadband performance verification of the phase shifter MMIC Type 1, measurements were conducted from 15 to 25 GHz. Figure 6 shows the measured insertion loss, relative phase shift range, and return losses. As seen from Figure 6, the measured relative phase shift range of $72 \pm 9°$, insertion loss variation of ± 0.2 dB, and return losses better than 15 dB were achieved from 15 to 25 GHz. Similarly, the simulation and measurement for MMIC Type 2 according to control voltages from 0 to 1.2 V are shown in Figure 7. The measured relative phase shift range of 104° and insertion loss of 2.4 ± 0.1 dB and return losses better than 20 dB were obtained at 21 GHz. Also, the broadband characteristic of the MMIC Type 2 is verified by the measured relative phase shift range of $96 \pm 8°$ with the constant insertion loss variation of ± 0.2 dB and return losses better than 15 dB were achieved from 17 to 25 GHz as shown in Figure 8. According to the measurement results for both MMIC's, Type 1 has smaller insertion loss and wider operation bandwidth because of the reduction in parasitic effect with respect to frequencies by compact size. Conversely, Type 2 has wider frequency tuning range by using a back-to-back connected diode as a varactor and slightly better consistency in loss by adopting a parallel resistor to minimize the loss variation. However, as the lack of linear variations in varactor capacitance in GaAs 0.15-μm low noise pHEMT process degrades linear phase variation with respect to control voltages for both types. Addition of another varactor diodes in reflective load with separate control voltage values applied to compensate the linearity of varactor diodes in reflection type phase shifter might be able to improve the linear phase variation.

The summarized performances of two broadband phase shifter MMIC's with constant loss variation are shown and compared with other GaAs reflection type phase shifters in Table 1. Although the other reflection type phase shifters cover 360° phase range, their better phase performances have been made in trade off with insertion loss and insertion loss variation due to the characteristics of reflection type phase shifters. Conversely, the presented Type 1 and Type 2 phase shifters emphasize the constant loss variation characteristics with moderate phase shift range over wide operation frequencies. That is, if the resonances of Type 1 and Type 2 are

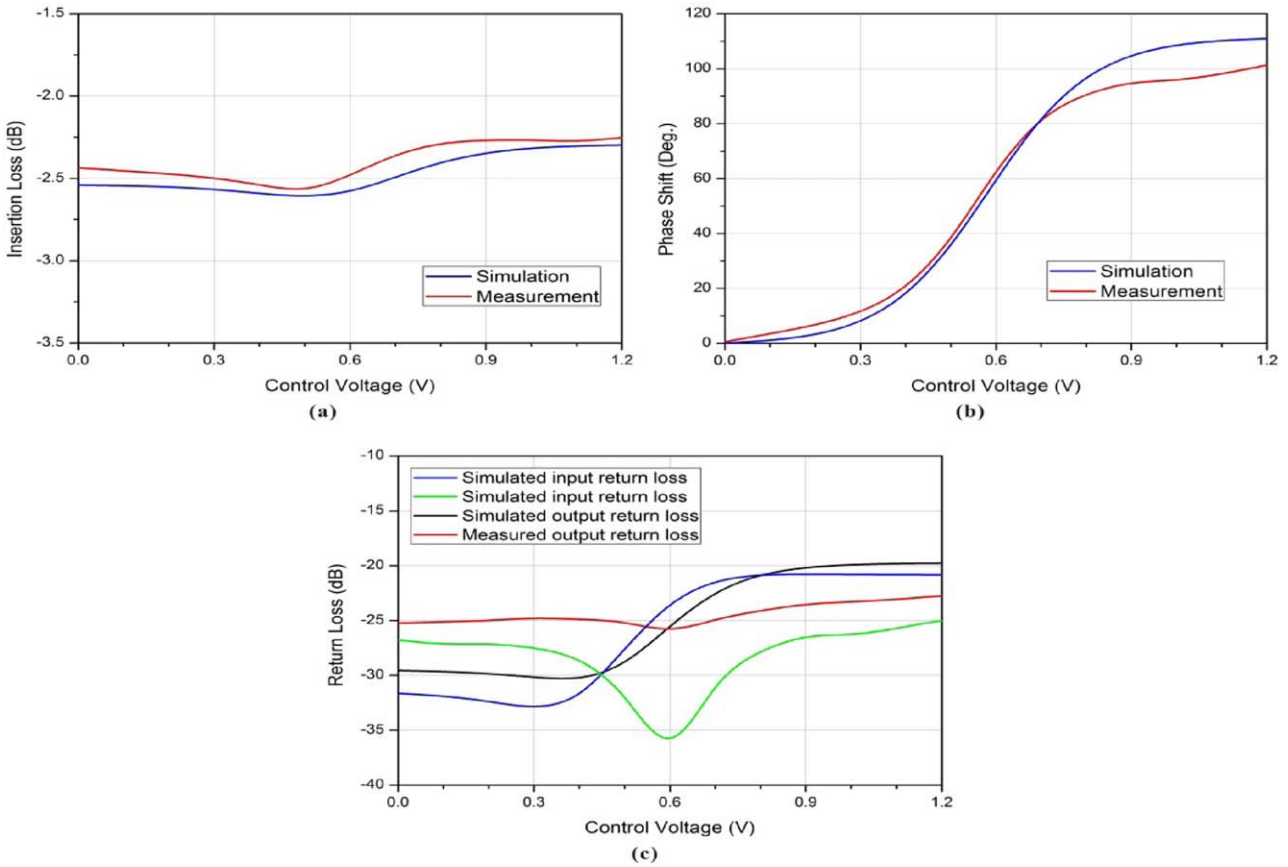

Figure 7 Simulated and measured (a) insertion loss, (b) relative phase shift range, and (c) input and output return losses for MMIC Type 2 at 21 GHz with control voltages from 0 to 1.2 V. [Color figure can be viewed in the online issue, which is available at wileyonlinelibrary.com]

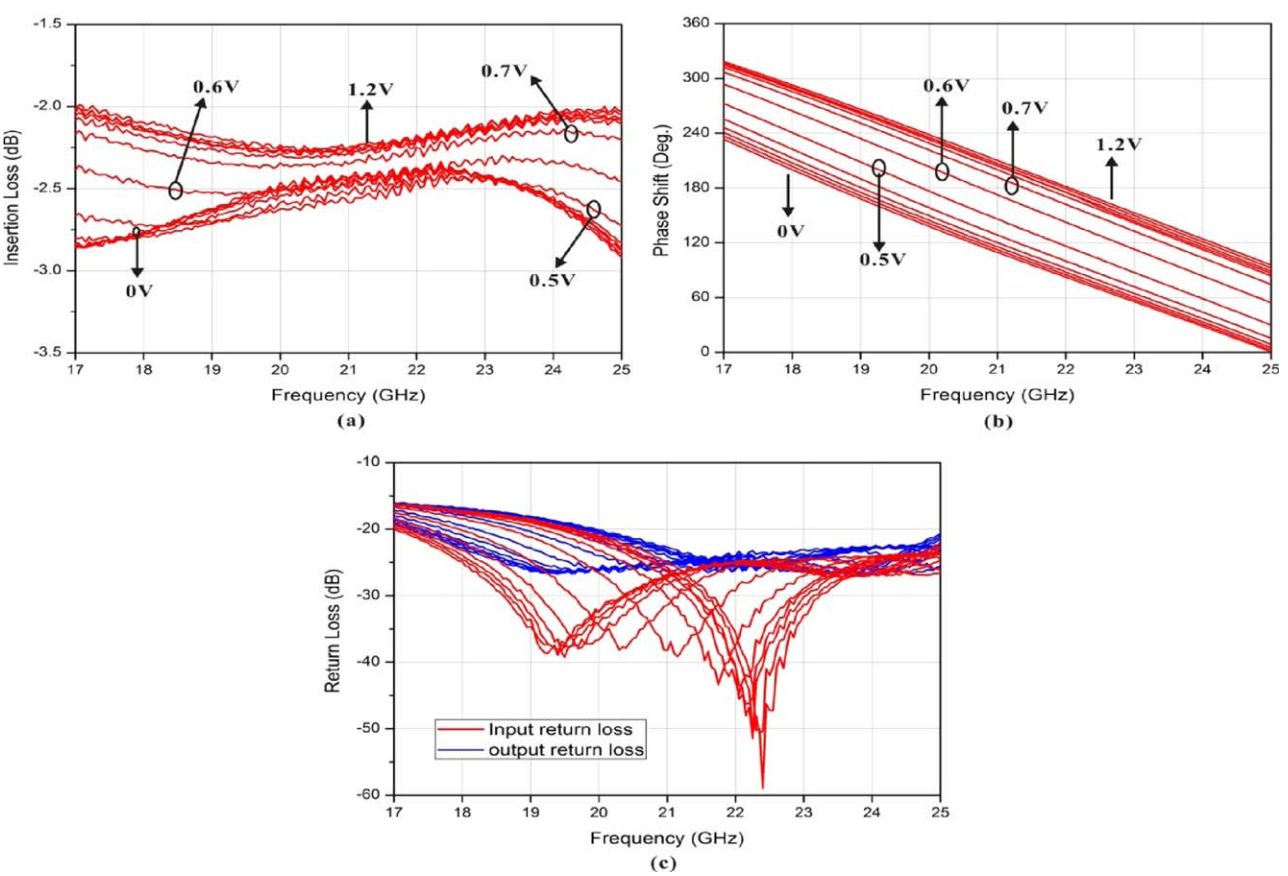

Figure 8 Measured (a) insertion loss, (b) relative phase shift range, and (c) input and output return losses for MMIC Type 2 from 17 to 25 GHz with control voltages from 0 to 1.2 V. [Color figure can be viewed in the online issue, which is available at wileyonlinelibrary.com]

TABLE 1 Comparisons of Monolithic Reflection Type Phase Shifters

Reference	Frequency (GHz)	Maximum Phase Range (°)	Insertion Loss (dB)	Insertion Loss Variation (dB)	Technique	Process
[1]	6.2	210	4.9	±0.9	Lumped-element coupler	0.6-μm GaAs
[7]	16–18	360	4.2	±0.9	Branch-line coupler with planar varactor	GaAs
[8]	8–12	90	1.5	±0.7	Optimized reflective circuitry	GaAs
[9]	5.15–5.7	360	6.4	±3.0	Two resonated loads in parallel	0.6-μm GaAs
Type 1	15–25	81	2.1	±0.2	Miniaturized Lange-coupler	0.15-μm GaAs
Type 2	17–25	104	2.4	±0.2	Addition of parallel balancing resistor	0.15-μm GaAs

tuned for maximum phase shift range rather than constant loss variation, the phase shift range could have been increase while the insertion loss characteristics would have been degraded. Despite there being difficulties in direct comparison with other reflection type phase shifters in Table 1, the presented Type 1 and Type 2 phase shifters show excellent performances in insertion loss, loss variation, and wideband characteristics, whereas the other reflection phase shifters have wider phase shift range. Depending on different requirements of various applications, phase shifters with constant insertion loss variation over wideband or phase shifters with wide phase shift range can be selected.

4. CONCLUSION

In this article, two types of compact broadband phase shifter MMIC's with constant insertion loss variations have been presented. Both phase shifters were configured to have constant insertion losses and implemented in GaAs 0.15-μm low noise pHEMT process. Type 1 phase shifter was designed with a miniaturized Lange coupler to have a minimum size and reduce parasitic losses. Type 2 phase shifter utilized a regular Lange coupler but adopts parallel resistor to minimize loss variation. Type 1 phase shifter had the measured relative phase shift range of 80° and insertion loss of 2.1 ± 0.2 dB at 20 GHz while the measured relative phase shift range of $72 \pm 9°$ and insertion loss variation of ±0.2 dB were achieved from 15 to 25 GHz. Type 2 phase shifter had the measured relative phase shift range of 104° and measured insertion loss of 2.4 ± 0.1 dB at 21 GHz. Also, the broadband characteristic of the second type was verified by the measured relative phase shift range of $96 \pm 8°$ with the constant insertion loss variation of ±0.2 dB from 17 to 25 GHz. Type 1 phase shifter with a miniaturization technique has shown a smaller frequency tuning range but an excellent performance over broadband freqeuncies, whereas Type 2 phase shifter has shown wider frequency tuning range and slightly better loss variation characteristics. Thus, the both types of phase shifters have been verified for the constant insertion loss variations and broadband characteristics at high frequencies.

ACKNOWLEDGMENT

This research was supported by Basic Science Research Program through the National Research Foundation of Korea (NRF) funded by the Ministry of Science, ICT & Future Planning (2012R1A1A2008310).

REFERENCES

1. F. Ellinger, R. Vogt, and W. Bächtold, Compact reflective-type phase-shifter MMIC for C-band using a lumped-element coupler, IEEE Trans Microwave Theory Tech 49 (2001), 913–917.
2. K.-O. Sun, C.-C. Yen, and D. Van der Weide, A size reduced reflection-mode phase shifter, Microwave Opt Technol Lett 47 (2005), 457–459.
3. H. Hayashi, T. Nakagawa, and K. Araki, A miniaturized MMIC analog phase shifter using two quarter-wave-length transmission lines, IEEE Trans Microwave Theory Tech 50 (2002), 150–154.
4. K. Miyaguchi, M. Hieda, K. Nakahara, H. Kurusu, M. Nii, M. Kasahara, T. Takagi, and S. Urasaki, An ultra-broad-band reflection-type phase-shifter MMIC with series and parallel LC circuits, IEEE Trans Microwave Theory Tech 49 (2001), 2446–2452.
5. C.-S. Lin, S.-F. Chang, C.-C. Chang, and Y.-H. Shu, Design of a reflection-type phase shifter with wide relative phase shift and constant insertion loss, IEEE Trans Microwave Theory Tech 55 (2007), 1862–1868.
6. C.-S. Lin, S.-F. Chang, and W.-C. Hsiao, A full-360° reflection-type phase shifter with constant insertion loss, IEEE Microwave Wireless Compon Lett 18 (2008), 106–108.
7. C.-L. Chen, W.-E. Courtney, L.-J. Mahoney, M.-J. Manfra, A. Chu, and H.-A. Atwater, A low-loss K-band monolithic analog phase shifter, IEEE Trans Microwave Theory Tech 35 (1987), 315–320.
8. S. Lucyszyn and I.-D. Robertson, Analog reflection topology building blocks for adaptive microwave signal processing applications, IEEE Trans Microwave Theory Tech 43 (1995), 601–611.
9. F. Ellinger, R. Vogt, and W. Bächtold, Ultra compact reflective-type phase shifter MMIC at C-band with 360 phase-control range for smart antenna combining, IEEE J Solid-State Circuits 37(2002), 481–486.

ANALYSIS ON SPECTRAL REGROWTH OF CHIRP BANDWIDTH EXPANSION TECHNIQUE IN HIGH-RESOLUTION SAR SYSTEM

Se Young Kim and Jin Bong Sung
Agency for Defense Development, P.O. Box 35-1, Daejeon 305-600, Korea; Corresponding author: sykim69888@daum.net

Received 7 June 2013

ABSTRACT: *This article presents an analysis of the root causes of the spectral regrowth due to the higher-order intermodulation in a chirp bandwidth expansion scheme using a single-sideband modulator and frequency multipliers. The spectral regrowth of synthetic aperture radar waveform was reduced by minimizing the gain and phase imbalances between the I and the Q channels. Further, the gain and phase imbalance requirements were defined on the basis of the evaluation of the impulse response function. The 150-MHz bandwidth of a chirp signal at 2.4 GHz was expanded to 600 MHz at 9.6 GHz. By adjusting the dc offset and the gain imbalance between the I and the Q channels, the carrier level was reduced from −28.7 to −53.4 dBm and the sidelobe levels caused by the spectral regrowth were reduced*